



Sustained delivery of VEGF from designer self-assembling peptides improves cardiac function after myocardial infarction

Hai-dong Guo^a, Guo-hong Cui^b, Jia-jun Yang^b, Cun Wang^c, Jing Zhu^a, Li-sheng Zhang^a, Jun Jiang^a, Shui-jin Shao^{a,*}

^a Department of Anatomy, School of Basic Medicine, Shanghai University of Traditional Chinese Medicine, Shanghai 201203, China

^b Department of Neurology, Shanghai No. 6 People's Hospital, Shanghai Jiaotong University School of Medicine, Shanghai 200233, China

^c Institutes of Biomedical Sciences, Fudan University, Shanghai 200032, China

ARTICLE INFO

Article history:

Received 25 May 2012

Available online 22 June 2012

Keywords:

Myocardial infarction

Angiogenesis

Transplantation

Self-assembling peptide

Cardiac tissue engineering

ABSTRACT

Poor vascularization and insufficient oxygen supply are detrimental to the survival of residual cardiomyocytes or transplanted stem cells after myocardial infarction. To prolong and slow the release of angiogenic factors, which stimulate both angiogenesis and vasculogenesis, we constructed a novel self-assembling peptide by attaching the heparin-binding domain sequence LRKKLGKA to the self-assembling peptide RADA16. This designer self-assembling peptide self-assembled into nanofiber scaffolds under physiological conditions, as observed by atomic force microscopy. The injection of designer self-assembling peptides can efficiently provide the sustained delivery of VEGF for at least 1 month. At 4 weeks after transplantation, cardiac function was improved, and scar size and collagen deposition were markedly reduced in the group receiving VEGF with the LRKKLGKA scaffolds compared with groups receiving VEGF alone, LRKKLGKA scaffolds alone or VEGF with RADA16 scaffolds. The microvessel density in the VEGF with LRKKLGKA group was higher than that in the VEGF with RADA16 group. TUNEL and cleaved caspase-3 expression assays showed that the transplantation of VEGF with LRKKLGKA enhanced cell survival in the infarcted heart. These results present the tailor-made peptide scaffolds as a new generation of sustained-release biomimetic biomaterials and suggest that the use of angiogenic factors along with designer self-assembling peptides can lead to myocardial protection, sufficient angiogenesis, and improvement in cardiac function.

© 2012 Elsevier Inc. All rights reserved.

1. Introduction

Despite encouraging proof-of-concept data suggesting that stem cell transplantation can improve post-infarct left ventricle (LV) function after myocardial infarction (MI), the efficacy of the procedure remains hampered by a low rate of sustained cell engraftment [1]. Poor vascularization may be the main factor contributing to graft attrition and the loss of residual cardiomyocytes. Several approaches toward enhancing angiogenesis and blood flow after MI have been investigated [2], including the use of various types of angiogenic factors, such as vascular endothelial growth factor (VEGF) [3] and fibroblast growth factor (FGF). VEGF165 gene delivery exerts a marked beneficial action by enhancing both arteriogenesis and cardiomyocyte viability in the infarcted myocardium [4]. Because small proteins can diffuse readily through the extracellular matrix, VEGF can signal over great distances, but this

property could restrict its retention within a tissue for prolonged periods. However, high doses of VEGF may lead to hemangioma, and the diffusion of VEGF may cause undesirable side effects [5].

To enable the specific targeting of angiogenic factors to the injured myocardium, growth factors have been delivered with a variety of natural matrices, such as gelatin, fibrin, collagen, and alginate, or synthetic materials including self-assembling peptides [6–10]. We have found that fibrin improves the results of stem cell transplantation to improve cardiac function by promoting angiogenesis [11]. The heparin binding delivery system sequestered the growth factors into a fibrin scaffold and limited their loss from the scaffold by diffusion [12]. Heparin-binding peptide amphiphile-based delivery of VEGF and FGF-2 to an omental transplant site significantly increased vascular density and improved islet engraftment [13]. However, natural biomaterials frequently contain residual growth factors, undefined constituents or non-quantified impurities.

Synthetic self-assembling peptides can create nanofiber microenvironments in the myocardium that promote vascular cell recruitment [14]. Recently, a class of designer self-assembling

* Corresponding author. Address: 1200 Cailun Road, Department of Anatomy, School of Basic Medicine, Shanghai University of Traditional Chinese Medicine, Shanghai 201203, China. Fax: +86 21 51322130.

E-mail address: shaoshuijin@163.com (S.-j. Shao).

peptides have also been functionalized through solid-phase synthetic extension with short functional sequences at their C- or N-termini [15]. We found that a designer self-assembling peptide incorporating the adhesion signal peptide RGDSP enhanced the adhesion, survival and differentiation of marrow-derived cardiac stem cells [16]. Tethering biotinylated insulin-like growth factor-1 (IGF-1) to biotinylated self-assembling peptides provided sustained IGF-1 delivery for 28 days and increased the survival of neonatal rat cardiomyocytes [17]. To date, the use of self-assembling peptides modified with bioactive peptides to bind and slowly release cytokines has not been reported. The heparin-binding delivery system provides a good foundation for the design of self-assembling peptides to promote the long-term release of angiogenic factors.

In this study, we first designed and synthesized a novel self-assembling peptide fused to the heparin-binding domain LRKKLGKA [18,19]. The goal was to achieve prolonged delivery of VEGF to enhance cardiac function recovery by promoting angiogenesis and preventing cardiomyocyte apoptosis. To evaluate the effects of VEGF delivery by the designer self-assembling peptide nanofibers, VEGF release and neovascularization were measured. LV contractile function, collagen deposition and scar area were also examined.

2. Materials and methods

2.1. Designer peptide synthesis and atomic force microscopy (AFM) observation

To achieve the effective delivery and release of growth factors, we modified the self-assembling peptide RADA16 (AcN-RADARA-DARADARADA-CONH₂) with one functional peptide motif, LRKKLGKA, to design a novel self-assembling peptide. LRKKLGKA has a strong binding affinity for heparin, which is then available to bind a wide variety of heparin-binding growth factors, including VEGF. The designer self-assembling peptide and RADA16 were custom synthesized. They were dissolved in sterile distilled water at a final concentration of 1% (w/v) (10 mg/ml) and sonicated for 30 min before use. The structures of the peptides were observed under AFM using the method described by Horii et al., [20].

2.2. Sustained delivery test of VEGF

To assess the feasibility of using designer self-assembling peptides for sustained VEGF delivery, we injected VEGF (Sigma) with self-assembling peptides or designer self-assembling peptides into the left ventricular myocardia of Sprague–Dawley (SD) rats (200–250 g, $n = 5$ in each group). The rats were placed under general anesthesia with ventilation, and the heart was exposed through a thoracotomy. The self-assembling peptides and designer self-assembling peptides were dissolved in sterile 295 mM sucrose at 1% (w/v) and sonicated for 30 min. An 80 μ l aliquot of VEGF (100 ng/rat), self-assembling peptides mixed with VEGF (100 ng VEGF/rat), or designer self-assembling peptides mixed with VEGF (100 ng VEGF/rat) and heparin (10 μ M, Sigma, sodium salt from porcine intestinal mucosa) was divided evenly and injected into each of four sites with a 28-gauge insulin syringe (20 μ l/injection), and the incision was closed. All animals received standard post-operative care, and the hearts were harvested after 1d, 7d, and 28d. For ELISA (anti-human VEGF ELISA, R&D System), proteins were extracted from the injected region using RIPA buffer supplemented with proteinase inhibitor cocktail and phosphatase inhibitor cocktail (Sigma).

2.3. Myocardial infarction model, transplantation and echocardiography

Female SD rats (200–250 g) were anesthetized with ketamine (40 mg/kg). Myocardial infarction was performed as described previously [11]. At 30 min after LAD ligation, the rats were randomly divided into control, VEGF alone, RADA16 alone, VEGF with RADA16, modified RADA16 (LRKKLGKA) alone and VEGF with LRKKLGKA groups. RADA16 and LRKKLGKA were dissolved in sterile sucrose (295 mM) at 1% (w/v) and sonicated for 20 min. In the VEGF with LRKKLGKA group, LRKKLGKA (80 μ l) with VEGF (100 ng) and heparin (10 μ M) were injected into 4 locations in the infarcted border zone (20 μ l for each injection). In the VEGF with RADA16 group, RADA16 (80 μ l) with VEGF (100 ng) were injected in the same way. PBS (80 μ l), VEGF (100 ng) in 80 μ l PBS, RADA16 (80 μ l), and LRKKLGKA (80 μ l) with heparin (10 μ M) were injected into the control, VEGF alone, RADA16 alone and LRKKLGKA alone rats, respectively. The chest was sutured after injection. Penicillin G benzathine (800,000 U per day) was given intramuscularly for three days after the operation. To evaluate the recovery of cardiac function, transthoracic echocardiography was performed at 4 weeks after injection [11].

2.4. Histological analysis

To detect fibrosis in the cardiac muscle, the hearts were excised, embedded in paraffin and stained with Masson's trichrome. The blue area was regarded as fibrotic tissue. Five different ventricular slices covering the infarcted area from the apex to the site of occlusion were scanned and computerized with a digital image analyzer (ImagePro Plus). Scar area was defined as the percentage of blue region in the cross-sectional area of whole myocardium in the LV wall, calculated using computer-based planimetry with ImageJ analysis software (NIH). Collagen volume fraction was calculated as the sum of all areas containing connective tissue divided by the total area of the image. The wall thickness of the infarct area was also measured using the image analyzer.

For histochemical analysis of microvessel density, 5 μ M tissue sections were prepared and stained with CD31 (BD Biosciences). After treatment with hydrogen peroxide to block endogenous peroxidase activity, the sections were incubated with mouse CD31 at 4 °C overnight, incubated with goat anti-mouse horseradish peroxidase-labeled secondary antibody and treated with 3,3'-diaminobenzidine. Finally, the nuclei were counterstained with hematoxylin. At least two microscopic fields in the peri-infarct regions were randomly selected and counted in three different sections from each animal. The results were expressed as the number of microvessels per 400 \times field.

2.5. Terminal dUTP nick-end labeling assay

Apoptosis was evaluated at 1 week after transplantation using the terminal deoxynucleotidyl transferase mediated dUTP nick end-labeling (TUNEL) assay (Chemicon, Temecula, California). The assay was performed according to the manufacturer's instructions, and nuclei were counterstained with 4',6'-diamidino-2-phenylindole. The degree of apoptotic cell death was determined by counting the total number of TUNEL-positive nuclei per microscopic field ($\times 400$).

2.6. Western blot analysis

The animals were sacrificed 1 week after transplantation. The hearts were explanted and immediately snap-frozen for Western blot studies. These samples were homogenized on ice in 0.1% Tween 20 homogenization buffer with a protease inhibitor. Then,

40 µg of protein was resolved by electrophoresis in a sodium dodecyl sulfate–polyacrylamide gel, and blotted onto a polyvinylidene fluoride membrane (Bio-Rad, Hercules, CA) overnight at 4 °C. The membranes were blocked in PBS buffer containing 0.2% Tween 20 and 5% nonfat milk for 2 h at room temperature. The blots were then incubated overnight at 4 °C with antibodies specific to caspase-3 and cleaved caspase-3 (Cell Signaling Technology, Beverly, MA, USA). Primary antibody binding was detected with an HRP-conjugated secondary antibody (Santa Cruz, San Francisco, CA) and visualized using an ECL kit. The ratio of cleaved caspase-3:total caspase-3 was compared between the groups using Quantity One software (Bio-Rad, Hercules, California).

2.7. Statistical analysis

Data are expressed as the means ± standard deviation. To analyze the data statistically, we performed a Student's *t* test and one-way analysis of variance (ANOVA) with Scheffe's post hoc multiple-comparison analysis. A value of *p* < 0.05 was considered to be statistically significant.

3. Results

3.1. Structures of designer self-assembling peptides

Upon the incorporation of a functional motif into the RADA16 peptide, there was some concern that the appended peptide motif would inhibit the nanofiber formation of the self-assembling peptide. To address this concern, we used AFM to examine the nanofiber structures of the designer peptides. AFM images revealed that the designer peptide can undergo spontaneous assembly into well-ordered nanofibers of ~10 nm in fiber diameter (Fig. 1A, B). Thus, the appended functional motif did not prevent peptide self-assembly.

3.2. Sustained delivery of VEGF by designer self-assembling peptides

When VEGF was injected with designer self-assembling peptides into the myocardium of rats, ~60% of the injected VEGF was retained in the injected region after 1 day. Only ~25% or ~12.5% of injected VEGF was retained at 1 day when injecting VEGF with or without non-modified self-assembling peptides, respectively. After 7 days, VEGF with or without non-modified self-assembling peptides disappeared rapidly, and only a small fraction of the injected VEGF was retained. In contrast, injected VEGF with designer self-assembling peptides was detected clearly. After 28 days, much more injected VEGF was detected in rats injected with both VEGF and designer self-assembling peptides, although injected VEGF with RADA16 could also be detected (Fig. 1C).

3.3. Improvement of LV contractile function

At 4 weeks after transplantation, the EF and FS in the five treatment groups were better than those in the control group. Echocardiographic examination showed that the EF and FS in the VEGF with RADA16 group (41.15 ± 4.30 and 26.67 ± 2.16) were higher than in the VEGF alone group (30.49 ± 3.48 and 19.51 ± 2.43 , *P* < 0.01) or the RADA16 alone group (28.49 ± 5.38 and 18.8 ± 2.96 , *P* < 0.01). The EF and FS in the VEGF with LRKKLGKA group (49.17 ± 3.73 , and 31.56 ± 3.10) were superior compared with those in the VEGF alone group, the LRKKLGKA alone group (32.49 ± 2.78 and 21.04 ± 2.23 , *P* < 0.01) and the VEGF with RADA16 group (*P* < 0.01) (Fig. 2A).

3.4. Infarct size, area of fibrosis and wall thickness of the infarct segment

At 4 weeks after transplantation, cross-sections at the mid-papillary muscle level showed transmural infarctions in all the animals. Semi-quantitative analysis demonstrated that the infarct size was significantly smaller in the VEGF with RADA16 group than

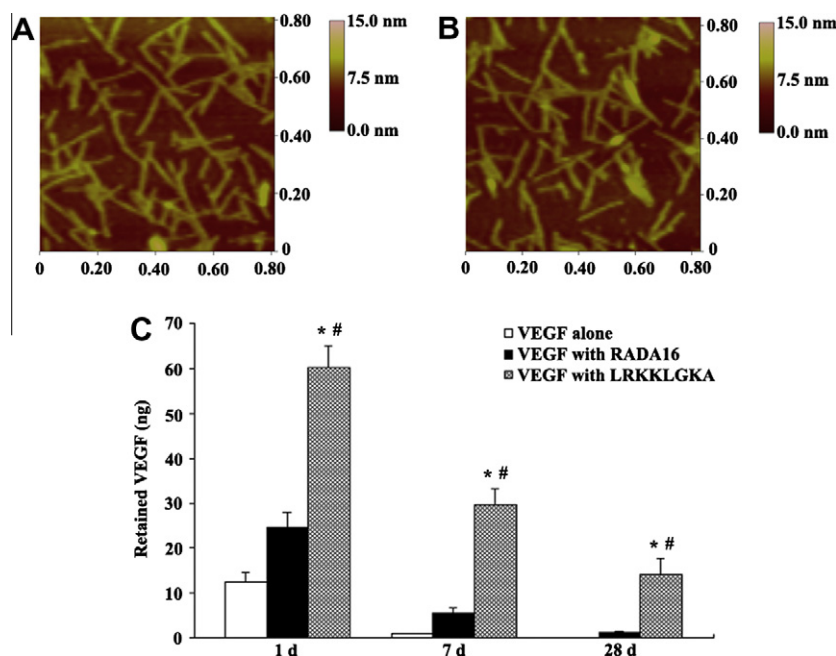


Fig. 1. Tapping Mode AFM images of peptides RADA16 (A) and LRKKLGKA (B) and retained VEGF at injected sites analyzed with human VEGF ELISA. The appended functional motif did not prevent peptide self-assembly. (C) Injection of designer self-assembling peptides can efficiently provide the sustained delivery of VEGF for 1 month. When VEGF was injected with or without RADA16, few or no growth factor molecules were detected at the injected sites at 28 days.

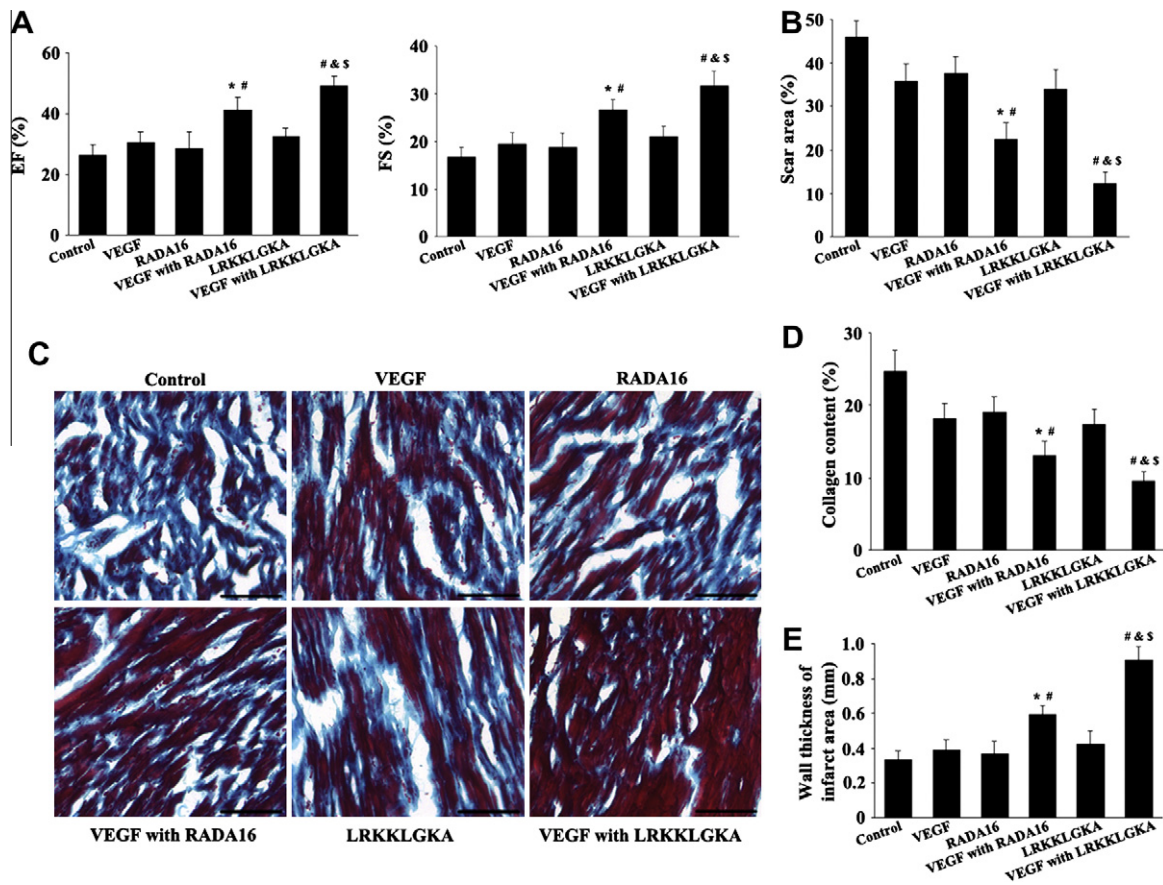


Fig. 2. Improvement of LV contractile function and histological changes at four weeks after transplantation. (A) EF (%) and FS (%) were compared among the different treatments. (B) Semi-quantitative analysis of myocardial infarct size. The rats in the VEGF with LRKKLGKA group showed the smallest infarct size. (C) Masson's trichrome for collagen deposition at 4 weeks after transplantation. Myocardium (red) was significantly replaced by fibrous tissue in the control group. A large number of cardiomyocytes were distributed among the collagen fibers in the infarction area in the VEGF with RADA16 and VEGF with LRKKLGKA groups. Scale bar = 100 μ m. (D) Quantitative analysis of the collagen volume fraction. (E) Quantitative analysis of infarct area wall thickness. ^{*} $P < 0.01$ versus the RADA16 group. [#] $P < 0.01$ versus the VEGF group. [&] $P < 0.01$ versus the LRKKLGKA group. ^S $P < 0.01$ versus the VEGF with RADA16 group; $n = 10$. (For interpretation of the references to colour in this figure legend, the reader is referred to the web version of this article.)

in the VEGF alone and RADA16 alone groups. Rats in the VEGF with LRKKLGKA group showed the smallest infarct size (Fig. 2B).

Masson's trichrome staining demonstrated obvious myocardial fibrosis in the control group. However, there was more regenerated myocardium in the infarction area in all treated groups at 4 weeks after transplantation. VEGF transplantation with LRKKLGKA scaffolds significantly attenuated the development of myocardial fibrosis relative to that observed in the other groups (Fig. 2C). Quantitative analysis demonstrated that the collagen volume fraction in the VEGF with LRKKLGKA group was significantly smaller than that in the VEGF alone group, the LRKKLGKA alone group or the VEGF with RADA16 group. Compared with the VEGF alone and RADA16 alone groups, the collagen content in the VEGF with RADA16 group was lower (Fig. 2D). The thickness of the old infarct wall was greater in VEGF with LRKKLGKA-treated rats than in the VEGF-treated, LRKKLGKA-treated and VEGF with RADA16-treated groups, although VEGF with RADA16 treatment increased the wall thickness of the infarct segment (Fig. 2E).

3.5. Angiogenesis

Angiogenic effect was determined by the number of CD31-positive microvessels observed at 4 weeks after transplantation. Representative images are shown in Fig. 3A. There was a significant increase in microvessel density in the VEGF alone, RADA16 alone, LRKKLGKA alone, VEGF with RADA16 and VEGF with LRKKLGKA

groups compared with the control group. The microvessel density in the VEGF with LRKKLGKA group was higher than that in the VEGF alone, LRKKLGKA alone, and VEGF with RADA16 groups. There were more microvessels in the VEGF with RADA16 group than in both the VEGF alone and RADA16 alone groups (Fig. 3B).

3.6. VEGF with modified RADA16 reduced apoptosis in infarcted myocardium

The expression of cleaved caspase-3 was significantly reduced in the infarcted heart in the VEGF with LRKKLGKA group than the VEGF alone, VEGF with RADA16, and LRKKLGKA alone groups at 1 week after transplantation (Fig. 4A, B). A significantly lower number of the TUNEL-positive nuclei were observed in the hearts of the VEGF with RADA16 groups compared with the VEGF alone and RADA16 alone groups. The number of TUNEL-positive nuclei in the VEGF with LRKKLGKA group was the lowest among the groups (Fig. 4C). Taken together, these data show that the transplantation of VEGF with LRKKLGKA enhanced cell survival in the infarcted heart.

4. Discussion

The heparin-binding domain of the designer peptide binds to heparin, which is then available to bind a wide variety of heparin-binding growth factors [12,19]. This is the premise of the

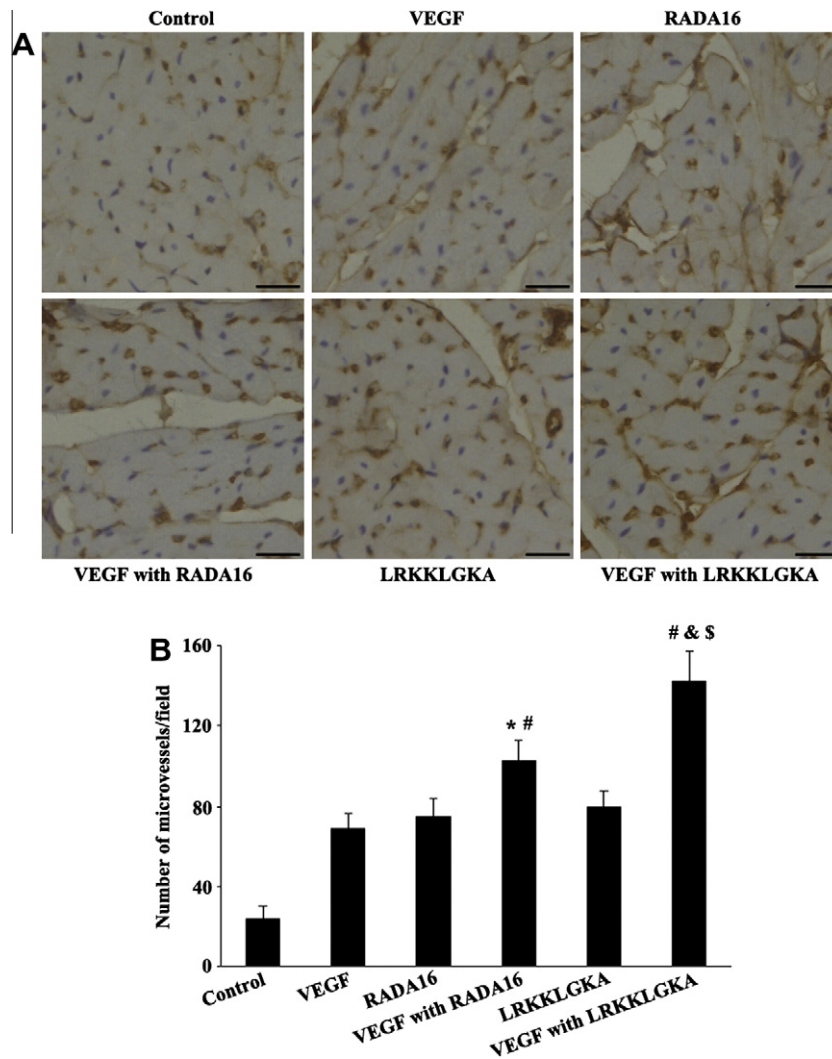


Fig. 3. Angiogenesis in the peri-infarct regions at 4 weeks after transplantation. (A) CD31 immunohistochemical staining. Compared with the control group, more microvessels were observed (brown) in all treated groups. Scale bar = 20 μ m. (B) Quantification of microvessel density. The microvessel density was significantly increased in the VEGF with RADA16 group compared with the RADA16 alone and VEGF alone groups. The microvessel density in the VEGF with LRKKLGKA group was higher than that in the VEGF with RADA16 group. * $P < 0.01$ versus the RADA16 group. # $P < 0.01$ versus the VEGF group. \$ $P < 0.01$ versus the LRKKLGKA group. $^{\$}P < 0.01$ versus the VEGF with RADA16 group; $n = 10$. (For interpretation of the references to colour in this figure legend, the reader is referred to the web version of this article.)

heparin-binding delivery system, which enables sequestered growth factors to be slowly released, such that release occurs primarily in response to cellular activity instead of by simple diffusion. Although RADA16 may adsorb growth factors through non-covalent interactions [21], RADA16 has no specific binding motif. Thus, we presumed that the delivery rates can be more precisely controlled by introducing binding motifs. In this study, we showed that the addition of a binding motif to the self-assembling peptide RADA16 did not inhibit its self-assembling properties or nanofiber formation. Based on this finding, a sustained VEGF delivery test was performed in the left ventricular myocardium of SD rats. After 7 days, VEGF disappeared rapidly, and only a small fraction of injected VEGF was retained in the injected region when VEGF was injected with or without RADA16. In contrast, VEGF injected with a designer self-assembling peptide was clearly detected. After 28 days, significantly more injected VEGF was detected in the hearts of rats injected with VEGF and the designer self-assembling peptides, although it could also be detected in rats injected with VEGF and RADA16. Therefore, the designer self-assembling peptides presented a long-term release pattern and exerted

long-lasting biological effects compared with RADA16 self-assembling peptides. This reduced infarct size and the apoptosis of cardiomyocytes, efficiently preserving cardiac function after MI.

VEGF is a key regulator of blood vessel formation during both angiogenesis and vasculogenesis. In our study, angiogenesis was determined by the number of CD31-positive microvessels at 4 weeks after transplantation. As demonstrated by David ED et al., self-assembling peptides recruit ECs and promote vascularization after injection into the myocardium. Our study showed that injection of RADA16 increased the number of CD31-positive microvessels. VEGF alone was less efficient in promoting angiogenesis and preserving cardiac function than VEGF loaded in self-assembling peptides and designer self-assembling peptides because much of the VEGF protein was washed away by body fluids. Because the angiogenic effect of VEGF is strongly dependent on its local concentration [22], VEGF used in conjunction with LRKKLGKA, as in the present study, may be favorable for the induction of angiogenesis. The microvessel density in the VEGF with LRKKLGKA group was higher than that in the LRKKLGKA alone and VEGF with RADA16 groups. The strong binding of VEGF to the LRKKLGKA

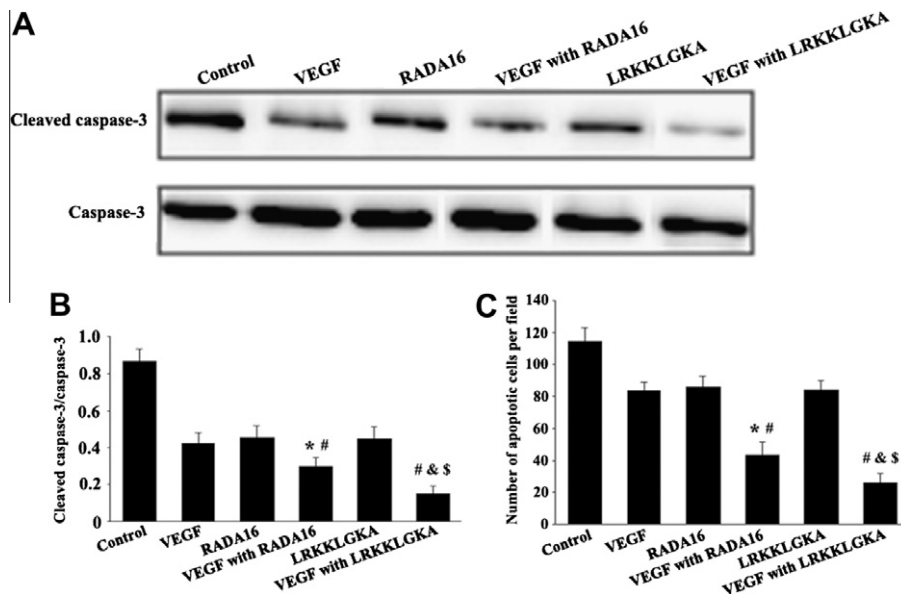


Fig. 4. VEGF with LRKKGKA reduced apoptosis in the infarcted myocardium. (A) Western blot evaluating cleaved caspase-3. At 1 week after transplantation, cleaved caspase-3 expression in the infarcted heart was significantly lower in the VEGF with LRKKGKA group than in the VEGF with RADA16 group. (B) Quantification of cleaved caspase-3 expression, normalized to caspase-3. (C) Quantification of TUNEL staining. * $P < 0.01$ versus the RADA16 group. # $P < 0.01$ versus the VEGF group. & $P < 0.01$ versus the LRKKGKA group. $^{\$}P < 0.01$ versus the VEGF with RADA16 group; $n = 10$.

increased the retention of VEGF and thus increased the angiogenesis. To establish more stable and functional vascular networks for the treatment of ischemic tissues, designer self-assembling peptides delivered in conjunction with more than one angiogenic factor, targeting both ECs and vascular smooth muscle cells, warrant further study.

The restoration of blood flow exerts beneficial effects on the survival of residual cardiomyocytes and prevents the progressive loss of cardiomyocytes. The expression of cleaved caspase-3 was significantly reduced in the infarcted heart in the VEGF with LRKKGKA group compared to the VEGF alone, VEGF with RADA16, and LRKKGKA alone groups at 1 week after transplantation. Furthermore, the fewest TUNEL-positive nuclei were observed in the VEGF with LRKKGKA. The transplantation of VEGF with LRKKGKA attenuated cell apoptosis in the infarcted heart by reducing the activation of caspase-3. Both the three-dimensional microenvironment supported by the designer self-assembling nanofiber scaffold itself and the sufficient blood flow generated from angiogenesis reduce apoptosis. Furthermore, VEGF might have a role in the recruitment or activation of a putative population of cardiac stem cells (CSCs) that could contribute to tissue repair after the onset of ischemia [23,24]. VEGF is critical for the spontaneous differentiation of stem cells into cardiomyocytes. Adipose-derived stem cells secrete significant amount of VEGF and that anti-VEGF receptor antibodies blocked cardiac differentiation [25]. VEGF also significantly increased cardiac-specific protein expression in differentiated embryonic stem cells [26]. Saving cardiomyocytes that are near death and recruiting or activating a putative population of CSCs increased the number of living cardiomyocytes. In the VEGF with LRKKGKA scaffold group, there was a great deal of living and newly regenerated myocardium in the infarction area. VEGF transplantation with LRKKGKA scaffolds significantly attenuated the development of myocardial fibrosis compared with the other groups. On the other hand, VEGF may exert a direct effect on cardiomyocyte contractility after its interaction with VEGFR1 and the consequent activation of PLC γ 1 [27]. Therefore, further studies are necessary to elucidate the desirable therapeutic effect after transplantation of the designer self-assembling peptides with angiogenic factors and stem cells.

Acknowledgments

This work was supported by grants from the Natural Science Foundation of China (Nos. 81102670 and 81072957), the Leading Academic Discipline Project of Shanghai Municipal Education Commission (J50301) and the Teacher Heritage Research Project of Shanghai University of Traditional Chinese Medicine (2009120).

References

- [1] C.J. Teng, J. Luo, R.C. Chiu, et al., Massive mechanical loss of microspheres with direct intramyocardial injection in the beating heart: implications for cellular cardiomyoplasty, *J. Thorac. Cardiovasc. Surg.* 132 (2006) 628–632.
- [2] S. Jiang, H.Kh. Haider, N.M. Idris, et al., Supportive interaction between cell survival signaling and angiocompetent factors enhances donor cell survival and promotes angiomyogenesis for cardiac repair, *Circ. Res.* 99 (2006) 776–784.
- [3] G.D. Yancopoulos, S. Davis, N.W. Gale, et al., Vascular-specific growth factors and blood vessel formation, *Nature* 407 (2000) 242–248.
- [4] M. Ferrarini, N. Arsic, F.A. Recchia, et al., Adeno-associated virus-mediated transduction of VEGF165 improves cardiac tissue viability and functional recovery after permanent coronary occlusion in conscious dogs, *Circ. Res.* 98 (2006) 954–961.
- [5] R.J. Lee, M.L. Springer, W.E. Blanco-Bose, et al., VEGF gene delivery to myocardium: deleterious effects of unregulated expression, *Circulation* 102 (2000) 898–901.
- [6] P.C.H. Hsieh, M.E. Davis, J. Gannon, et al., Controlled delivery of PDGF-BB for myocardial protection using injectable self-assembling peptide nanofibers, *J. Clin. Invest.* 116 (2006) 237–248.
- [7] X. Hao, E.A. Silva, A. Mansson-Broberg, et al., Angiogenic effects of sequential release of VEGF-A165 and PDGF-BB with alginate hydrogels after myocardial infarction, *Cardiovasc. Res.* 75 (2007) 178–185.
- [8] J. Zhang, L. Ding, Y. Zhao, et al., Collagen-targeting vascular endothelial growth factor improves cardiac performance after myocardial infarction, *Circulation* 119 (2009) 1776–1784.
- [9] Z.Q. Shao, K. Takagi, Y. Katayama, et al., Effects of intramyocardial administration of slow-release basic fibroblast growth factor on angiogenesis and ventricular remodeling in a rat infarct model, *Circ. J.* 70 (2006) 471–477.
- [10] J.H. Kim, Y. Jung, S.H. Kim, et al., The enhancement of mature vessel formation and cardiac function in infarcted hearts using dual growth factor delivery with self-assembling peptides, *Biomaterials* 32 (2011) 6080–6088.
- [11] H.D. Guo, H.J. Wang, Y.Z. Tan, et al., Transplantation of marrow-derived cardiac stem cells carried in fibrin improves cardiac function after myocardial infarction, *Tissue Eng. Part A* 17 (2011) 45–58.

- [12] S.J. Taylor, E.S. Rosenzweig, J.W. McDonald 3rd., et al., Delivery of neurotrophin-3 from fibrin enhances neuronal fiber sprouting after spinal cord injury, *J. Controlled Release* 113 (2006) 226–235.
- [13] J.C. Stendahl, L.J. Wang, L.W. Chow, et al., Growth factor delivery from self-assembling nanofibers to facilitate islet transplantation, *Transplantation* 86 (2008) 478–481.
- [14] M.E. Davis, J.P. Motion, D.A. Narmoneva, et al., Injectable self-assembling peptide nanofibers create intramyocardial microenvironments for endothelial cells, *Circulation* 111 (2005) 442–450.
- [15] E. Genové, C. Shen, S. Zhang, et al., The effect of functionalized self-assembling peptide scaffolds on human aortic endothelial cell function, *Biomaterials* 26 (2005) 3341–3351.
- [16] H.D. Guo, G.H. Cui, H.J. Wang, et al., Transplantation of marrow-derived cardiac stem cells carried in designer self-assembling peptide nanofibers improves cardiac function after myocardial infarction, *Biochem. Biophys. Res. Commun.* 399 (2010) 42–48.
- [17] M.E. Davis, P.C. Hsieh, T. Takahashi, et al., Local myocardial insulin-like growth factor 1 (IGF-1) delivery with biotinylated peptide nanofibers improves cell therapy for myocardial infarction, *Proc. Natl. Acad. Sci. USA* 103 (2006) 8155–8160.
- [18] K. Rajangam, H.A. Behanna, M.J. Hui, et al., Heparin binding nanostructures to promote growth of blood vessels, *Nano Lett.* 6 (2006) 2086–2090.
- [19] T.A. Ahmed, E.V. Dare, M. Hincke, Fibrin: a versatile scaffold for tissue engineering applications, *Tissue Eng. Part B Rev.* 14 (2008) 199–215.
- [20] A. Horii, X. Wang, F. Gelain, et al., Biological designer self-assembling peptide nanofiber scaffolds significantly enhance osteoblast proliferation, differentiation and 3-D migration, *PLoS One* 2 (2007) e190.
- [21] V.F.M. Segers, R.T. Lee, Local delivery of proteins and the use of self-assembling peptides, *Drug Discov. Today* 12 (2007) 561–568.
- [22] S. Yla-Herttuala, T.T. Rissanen, I. Vajanto, et al., Vascular endothelial growth factors: biology and current status of clinical applications in cardiovascular medicine, *J. Am. Coll. Cardiol.* 49 (2007) 1015–1026.
- [23] A. Linke, P. Müller, D. Nurzynska, et al., Stem cells in the dog heart are self-renewing, clonogenic, and multipotent and regenerate infarcted myocardium, improving cardiac function, *Proc. Natl. Acad. Sci. USA* 102 (2005) 8966–8971.
- [24] K. Urbanek, D. Torella, F. Sheikh, et al., Myocardial regeneration by activation of multipotent cardiac stem cells in ischemic heart failure, *Proc. Natl. Acad. Sci. USA* 102 (2005) 8692–8697.
- [25] Y.H. Song, S. Gehmert, S. Sadat, et al., VEGF is critical for spontaneous differentiation of stem cells into cardiomyocytes, *Biochem. Biophys. Res. Commun.* 354 (2007) 999–1003.
- [26] Y. Chen, I. Amende, T.G. Hampton, et al., Vascular endothelial growth factor promotes cardiomyocyte differentiation of embryonic stem cells, *Am. J. Physiol. Heart Circ. Physiol.* 291 (2006) H1653–H1658.
- [27] W. Rottbauer, S. Just, G. Wessels, et al., VEGF-PLC gamma1 pathway controls cardiac contractility in the embryonic heart, *Genes Dev.* 19 (2005) 1624–1634.